Delft University of Technology

Understanding piezoelectric composite–based actuators with nonlinear and 90 domain walls effects

Wiwattananon, Peerawan; Bergsma, Otto; Bersee, Harald

Important note
To cite this publication, please use the final published version (if applicable).
Please check the document version above.

Understanding piezoelectric composite–based actuators with nonlinear and 90° domain walls effects

Peerawan Wiwattananon, Otto K Bergsma and HEN Bersee

Abstract

Piezoelectric materials possess nonlinear behavior when actuated in a large electric field and show a large deflection when embedded inside a composite laminate such as a LIghtweight Piezoelectric Composite Actuator. Linear and nonlinear COMSOL multi-physics finite element models were developed and validated using the actuation response of three different layups of LIghtweight Piezoelectric Composite Actuators under a cantilever beam configuration. The linear model incorporated the linear piezoelectric coefficient given from the manufacturer, while the nonlinear model incorporated the nonlinear piezoelectric coefficient plus permanent strain offset in the piezoelectric material as a result of a high applied electric field. The linear model significantly underestimated the experimental values of the actuator response and it showed that taking nonlinearity and permanent strain offset into account is an essential practice when an actuator is operated in high electric fields and accurate prediction is required.

Keywords

actuator, piezoelectric, active composites, piezoceramics

Introduction

The LIghtweight Piezoelectric Composite Actuator (LIPCA) (Goo et al., 2001) was developed in an attempt to find a lighter alternative to the metallic THin layer composite UNimorph ferroelectric DrivER and sensor (THUNDER) (Antcliff and McGowan, 2001; Mossi et al., 1998). The LIPCA systems are composed of a piezoelectric layer embedded in a low coefficient of thermal expansion (CTE) carbon layer and higher CTE base glass layers. As with THUNDER, residual stresses arise during the curing process due to a mismatch in CTE of the constituent layer together with the unsymmetrical laminate, resulting in the curved shape of the LIPCA (Goo et al., 2001; Yoon et al., 2002).

Since piezoelectric materials produce a small strain when an electric field is applied, a large electric field range is needed to obtain a large desirable strain. Hence, the effect of the nonlinear strain–electric field response inside the piezoelectric material increases, as well as the permanent strain offset that is developed as soon as the piezoelectric material has gone through a high electric field. The nonlinear phenomenon is a result of the extrinsic effect inside the piezoelectric due to a high electric field (Li et al., 1991; Pramanick et al., 2009, 2011); the permanent strain is a result of the inability of the piezoelectric domain walls to entirely reorient back to their initial state after being oriented by a high electric field especially, opposing the poling direction (Pramanick et al., 2009, 2011).

Before extrinsic and permanent strain offset are illustrated, a simple strain–electric field response known as piezoelectric effect is introduced. Figure 1(a) illustrates randomly oriented domains and domain walls inside a bulk piezoelectric material before the piezoelectric material is poled. At this stage, the piezoelectric material possesses no piezoelectric effect unless it is poled. The piezoelectric material is poled by an introduction of a large electric field to the bulk piezoelectric material until the domains and the domain walls orient according to the electric field (Figure 1(b)). The piezoelectric effect is described as a response of the domain walls according to a low magnitude of applied electric field causing small and linear output strain (Li et al., 1997).

Structural Integrity and Composites, Faculty of Aerospace Engineering, Delft University of Technology, Delft, The Netherlands

Corresponding author:
Peerawan Wiwattananon, Structural Integrity and Composites, Faculty of Aerospace Engineering, Delft University of Technology, Kluyverweg 1, 2629 HS Delft, The Netherlands.
Email: peerawan.wiwattananon@nasa.gov

The domain walls move with the electric field and are able to orient back to their initial state (Figure 1(c)). The extrinsic effect can be described as a nonlinear response of the 90° domain walls, or sometimes called non-180° domain walls, to a large applied electric field resulting in large magnitudes of nonlinear output strain (Hall, 2001). When large magnitudes of electric field are enough to cause permanent 90° domain wall orientations, permanent strain offset will be produced in the piezoelectric material (Figure 1(d)). These phenomena can be considered as a small effect when it stays at a piezoelectric scale, but once they are amplified by a unimorph-type actuator, the phenomena can cause significant impact on the actuator's accuracy.

Within this study, three different LIPCA layups are manufactured and statically actuated under a direct current (DC) electric potential up to the piezoelectric material nonlinear range. In order to study the actuator behavior under separated applied DC polarities, the positive and negative electric potentials were applied separately and investigated. When applying the actuator in the piezoelectric material's nonlinear range, good actuation predictions are essential when actuation effects are sensitive to high accuracy. Moreover, a permanent displacement offset in an actuator's level, resulting from a permanent strain offset developed in the piezoelectric material, could become significant to the application; therefore, this phenomenon needs to be detected and understood.

Two finite element models linear and nonlinear models were developed and compared results obtained experimentally. The former comprised a linear piezoelectric coefficient provided by the manufacturer, while the latter took nonlinear piezoelectric coefficients and permanent strain offsets from the piezoelectric material into account. The nonlinear piezoelectric coefficients and permanent strain offsets were determined experimentally. The comparisons between the experimental results and the models and the actuator performance between different layups are discussed below.

Finite element model

Two-dimensional (2D) models of three different layups of LIPCAs, that is, [G/PZT/G/C], [G/PZT/G/G/C], and [G/PZT/G/C/G/C] were developed using a COMSOL Multiphysics version 4.2. "G" refers to a glass layer, "C" refers to a unidirectional carbon layer and "PZT" refers to a piezoelectric layer. [G/PZT/G/C] represents a stacking sequence according to the composite laminate convention. The 2D model was enough to describe the actuation behavior because the width of these actuators is narrow so that the width will not influence to the actuation response. If the actuators are a beam-like type actuator, that is, aspect ratio is less than 0.33; the actuator will not exhibit a snap-through
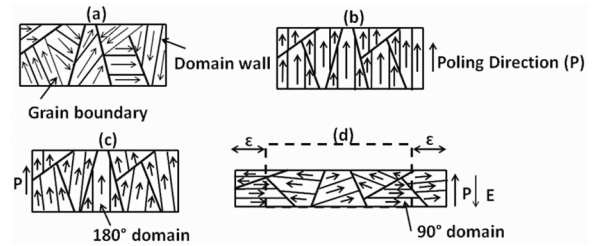
Figure 1. (a) Illustrates randomly oriented domain and domain walls in the bulk piezoelectric material before being poled. The arrows represent the direction of the domain inside the piezoelectric material, (b) illustrates the bulk piezoelectric material is being poled with domains and domain walls oriented along with the poling direction, denoted "P," (c) a poled bulk piezoelectric material resulting in 180° domain wall orientations, same direction as the poling direction. Note that some domains are slightly reoriented back to their original orientation but still in a favor of the poling direction. The poled piezoelectric is now ready for applications. During a small magnitude input electric field, the domain walls rotate with respect to the electric field and are able to orient back to their original state; (d) illustrates 90° domain wall orientations when the bulk piezoelectric material experiences a large magnitude of electric field opposing the poling direction resulting in permanent strain offset, denoted "ε." The dashed block represents the original size of the piezoelectric material before a large magnitude electric field was applied.
Source: Adapted from Ballas (2007).

effect during actuation (Aimmanee and Hyer, 2006). Note that all the actuators used in this study possessed an aspect ratio of 0.32. If an actuator exhibits a snap-through effect, for example, a plate-like actuator, then a 2D model might not be capable to describe the actuation behavior well enough because the actual largest actuation displacement might move to different locations along the width during the snap-through effect. If this is the case, then modeling the actuators using a three-dimensional (3D) model is necessary to capture all the possible largest actuation displacement locations. Moreover, the authors believe that the 2D model can represent the 3D model well in this case. This is because of the material properties of a unidirectional carbon layer along the width is different from the lengthwise. This leads to a difference in the neutral axis locations as can be observed in Figure 2. Considering the locations of the neutral axis of each actuator layup along the lengthwise, as shown in the figure, when compared to the neutral axis of each layup along the width-wise, the neutral axis locations of each layup along the length shift toward the top face of the PZT layer more than those along the width-wise. This is because the stiffness value of the carbon layer along the width-wise is a matrix dominant; the stiffness is much lower along the width of the carbon layer when compared to its length, and this makes the carbon layer dominate less to the actuator's stiffness along the width than the length
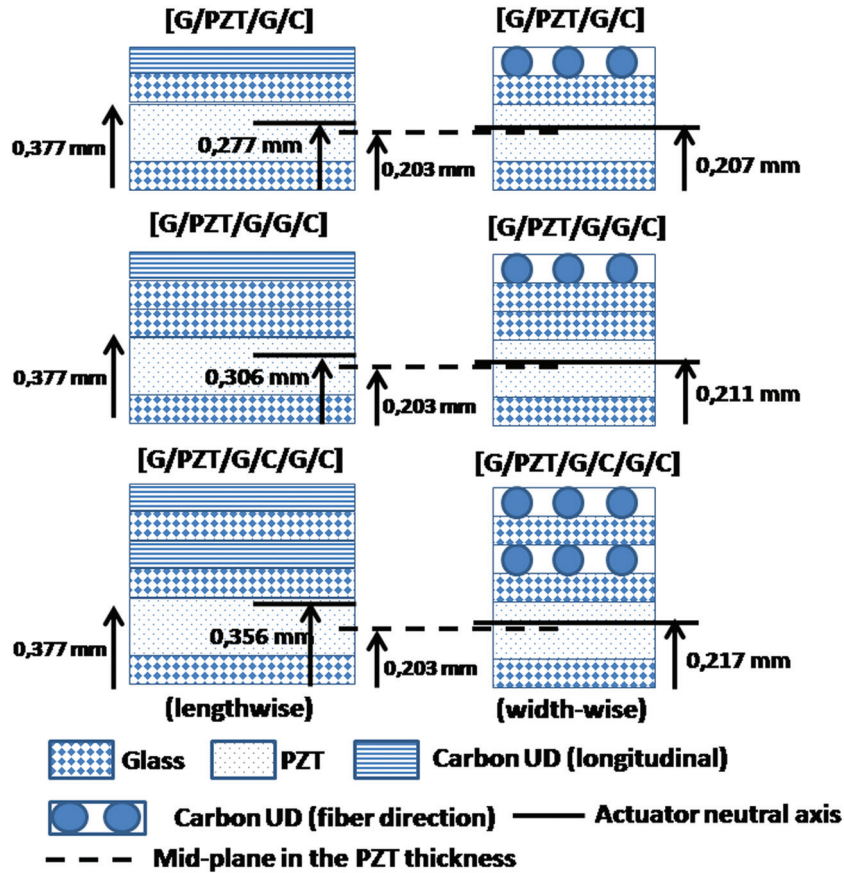
Figure 2. Neutral axis locations along the actuators' length and width. The neutral axis along the longitudinal (lengthwise) varies more than along the transverse (width-wise) direction because of the elastic modulus of a carbon layer is higher along the longitudinal axis while the carbon layer is matrix dominant along the transverse direction.

direction. Thus, the neutral axis of the actuators will not move further away from the mid-plane of the PZT layer much when compared to the neutral axis along the lengthwise. This leads to smaller bending moment created during actuation from the actuator's width when compared to the actuator's length. Therefore, the initial strain along the actuator's width should not play a major role in the actuation displacement.

The 2D model comprises two sub-models with two different consecutively coupled physics. The first sub-model computes the manufactured shape after the LIPCA has gone through the manufacturing process using a "solid mechanics" physics. The second sub-model computes the actuation displacements of the LIPCA when configured under a cantilever beam configuration while electric potential is applied to the LIPCA. The second physics is "piezoelectric device" interface. An example of the model dimensions for [G/PZT/G/C] for both manufactured shape and actuation response is shown in Figure 3.

The dimensions of the materials inside the model of the LIPCA were the following. The glass layers were 75 mm × 70 μm (length × thickness), the carbon layer was 75 mm × 72 μm, and the PZT dimension
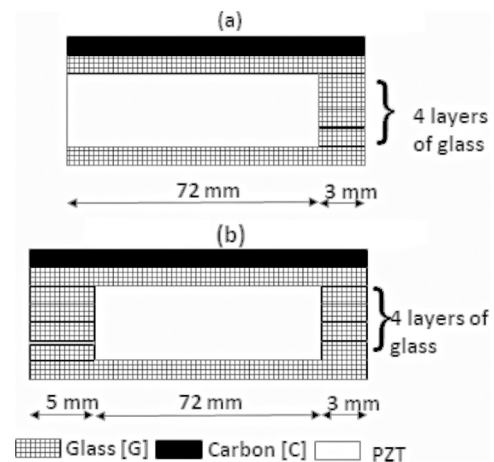
Figure 3. (a) Represents the model dimension of the LIPCA [G/PZT/G/C] used in this study and (b) the actual actuator dimension of [G/PZT/G/C].

was 72 mm × 267 μm. To compensate the PZT's thickness, four layers of glass, 3 mm × 66.75 μm each layers, were applied at the right end. While within the actual LIPCA the glass layers were 80 mm × 70 μm and the carbon layer was 80 mm × 72 μm. The left

Properties	Glass fabric GEP 108	Carbon UD USN075B	PZT (5A4E)
E_1, E_3 (GPa)	21.7, 4	128.32, 4	66, 52
G_{13} (GPa)	3.99	2.5	–
α_1 and α_3 (1×10^{-6}/K)	14.2, 0	-6.25, 0	4, 4
Poisson ratio, ν_{12}, ν_{13}	0.13, 0.13	0.3, 0.3	0.3, 0.3
Density (kg/m^3)	1800	1120	7800
Thickness (μm)	70	72	267
Linear d_{31}, d_{33} (pm/V)	–	–	-190, 390
Manufacturer	SK Chemicals, Korea	SK Chemicals, Korea	Piezo System, Inc., USA

glass tab was 5 mm $\times$ 70 μm and the right was 3 mm $\times$ 70 μm as shown in Figure 3(b). The total thickness of the four layers of glass at the tabs exceeds the piezoelectric thickness before curing but the total thickness of these tabs was reduced due to a high applied pressure during the curing process, while the piezoelectric material's thickness remains unchanged. To simplify the model, two sub-models were combined into one with reduced dimensions representing the cantilever beam configuration (Figure 3(a)). In this way, the cantilever configuration of both model and the actual one were identical. The model and actual dimensions for other two layups, [G/PZT/G/G/C] and [G/PZT/G/C/G/C], are similarly developed. The actuator was clamped at the 5-mm tab during actuation; to combine the two sub-models into one, the model had the total length of 75 mm instead of 80 mm, keeping the cantilever beam span length of the model identical to the experiment. The material properties applied in this model are given in Table 1, α_1 and α_3 are CTE along the 1 and 3-directions, respectively, ν_{12} and ν_{13} represent the Poisson's ratios along the 1–2 and 1–3 directions, respectively. G_{13} is a shear modulus along the 1–3 direction.

Manufactured shape: solid mechanics physics (solid)

The manufactured shape of an actuator took into account the thermal effects of different materials due to the differences in the CTEs of different materials. The stresses resulted from the fact that most of the residual stresses began to build up in the composite laminate at the temperature lower than the curing temperature, which was the glass transition temperature (Jeronimidis and Parkyn, 1988). The temperature higher than the glass transition temperature was the stress-free temperature (Jeronimidis and Parkyn, 1988). If the curing temperature is taken into account as the initial temperature then there will be an overestimate of the residual stress. Therefore, the initial temperature used was not the material curing temperature (125°C) but rather the glass transition temperature of 112.72°C, given by the manufacturer, and the final temperature was the room temperature (25°C). To predict the manufactured
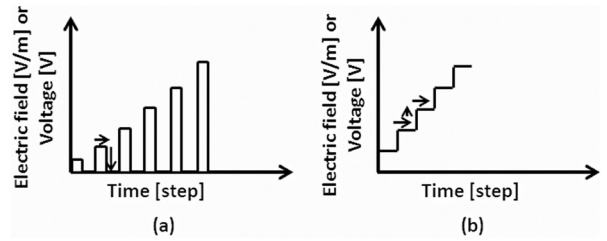
Figure 4. Two schematics of the applications of electric field or voltage through the arrows: (a) application of the electric field or voltage for a particular time step then it is discharged to a zero electric field before the application of the next higher field level and (b) application of the electric field or voltage without discharging.

shape of the actuators, the boundary condition was simply-supported to allow free deformation of the actuator resulting in considerable curvature.

Actuation displacement: piezoelectric device physics (pzd)

The thermal stress developed from the previous manufacturing step influenced the actuation response in the second step. Therefore, the thermal stress resulting from the thermal effect was transferred to the second step, piezoelectric device physics. The plane stress was again assumed similar to the solid mechanics physics. Two different actuation response models were investigated: the linear model which comprises a linear piezoelectric coefficient, d_{31}, provided by the manufacturer as shown in Table 1 and the nonlinear model which incorporated experimentally determined nonlinear piezoelectric coefficient, $d_{31nonli}$, plus the permanent strain offset inside the piezoelectric material. To replicate the actual situation of the piezoelectric material embedded in the composite laminate, the nonlinear piezoelectric coefficient was obtained when the piezoelectric patch was discharged prior to applying the next higher electric field, while the strain state was un-tuned back to its zero strain to allow the permanent residual strain to maintain inside the piezoelectric material

(Figure 4(a)). The LIPCAs possess extension-bending coupling due to an asymmetric layup that can result in a large out-of-plane cylindrical curved shape after manufacturing (Goo et al., 2001; Yoon et al., 2002). The actuation displacement of the LIPCA is very large, that is, larger than its thickness; therefore, geometric nonlinearity was taken into account in these analysis. The geometrically linear theory has been shown to be incapable to predict the actuation displacement of such actuators when actuated at large input electric potential (Aimmanee and Hyer, 2006). This is because the geometrically linear theory does not take into account the out-of-plane displacement, along the out-of-plane direction such as a z-direction, with respect to the in-plane direction such as x and y directions, that is, all the underlined terms in equation (1). To take into account the out-of-plane displacement, w^0, with respect to the in-plane direction, the two sub-models must take geometric nonlinearity into account (Aimmanee and Hyer, 2006). The reference surface strains, ε_x^0, ε_y^0, and γ_{xy}^0, taking into account the geometric nonlinearity are shown in equation (1) (Aimmanee and Hyer, 2006). For the geometrically linear analysis, the underline terms are not included (Aimmanee and Hyer, 2006). u^0 and v^0 represent in-plane displacement

$$
\begin{aligned}
\varepsilon_x^0 &= \frac{\partial u^0}{\partial x} + \underline{\frac{1}{2}\left(\frac{\partial w^0}{\partial x}\right)^2} \\
\varepsilon_y^0 &= \frac{\partial v^0}{\partial y} + \underline{\frac{1}{2}\left(\frac{\partial w^0}{\partial y}\right)^2} \qquad (1) \\
\gamma_{xy}^0 &= \left(\frac{\partial u^0}{\partial y} + \frac{\partial v^0}{\partial x}\right) + \underline{\left(\frac{\partial w^0}{\partial x}\right)\left(\frac{\partial w^0}{\partial y}\right)}
\end{aligned}
$$

Manufacturing and experimental setup

LIPCAs with three different layups were manufactured for this study with the dimensions 80-mm long × 26-mm wide. The glass fabric epoxy prepreg, carbon UD epoxy prepreg, and a piezoelectric material patch were stacked together (Wiwattananon et al., 2009) and copper foils were used as the electric power inlet. The stacked LIPCA was positioned between two flat stainless steel plates and the whole setup cured in a hot press. The curing cycle was performed at a pressure of 3 bars and a temperature of 125°C (Wiwattananon et al., 2011) for 3 h.

The LIPCA was clamped pointing upward perpendicularly to the table making a span length of 75 mm. The actuation displacements were measured using a non-contact laser beam measurement system at the tip of the LIPCA. The LIPCA was actuated by the input electric potential through the copper foils. Two different electric potential applications were investigated in this study, that is, each actuator was actuated under the non-discharging condition followed by a

discharging condition. Within each charging condition, the actuators were applied with a DC positive potential starting from 0 to + 200 V with + 10 V increment. The actuator was discharged by 0 V and was consecutively applied using a negative DC potential starting from 0 to −200 V in −10 V steps. The discharging condition refers to the procedure that the actuator was being discharged, a 0 V applied, prior to the next input electric potential (Figure 4(a)). The non-discharging condition refers to the procedure where the actuator is not discharged prior the next higher electric potential (Figure 4(b)). In order to ensure the consistency of the excitation, each excitation set was repeated 4–5 times and the results were averaged.

Nonlinear piezoelectric coefficients

The nonlinear piezoelectric coefficients were determined experimentally by applying a unipolar DC electric field to a bulk piezoelectric material. Positive and negative DC electric fields were separately applied to the piezoelectric material. The piezoelectric material was discharged before the next higher electric field was applied, under similar testing condition as those shown in Figure 4(a), and the residual strain state inside the piezoelectric material was allowed to remain inside a piezoelectric material. The residual strain was allowed to remain inside the piezoelectric material in order to replicate the actual behavior of the piezoelectric material, that is, being unable to expand and contract freely, when embedded inside a composite laminate. The residual strain is shown as an offset of the strain at a zero field in Figure 5. The nonlinear piezoelectric coefficient, denoted $d_{31nonli}$, of each unipolar were derived from equation (2) (Standards Committee of the IEEE Ultrasonics, Ferroelectrics, and Frequency Control Society, 1988) and are tabulated in Table 2. The "ε" is a strain and the term "E" is an input electric field

$$
d_{31nonli} = \frac{\partial \varepsilon}{\partial E} \qquad (2)
$$

It can be observed that the bulk piezoelectric material used to make actuators in this study showed nonlinear output in-plane strains under both DC electric field polarities. It is clear that the negative electric field exhibited a larger initial strain offset than the positive field and a larger strain at higher electric fields. The piezoelectric material experienced a permanent strain offset when a large magnitude electric field was enough to cause permanent 90° domain wall orientations. The irreversibility of the 90° domain walls was more prone in the applied electric field opposing to the polarization direction. The phenomenon of irreversible 90° domain wall orientations were more obvious under the negative electric field (Figure 5(a)) than under the positive
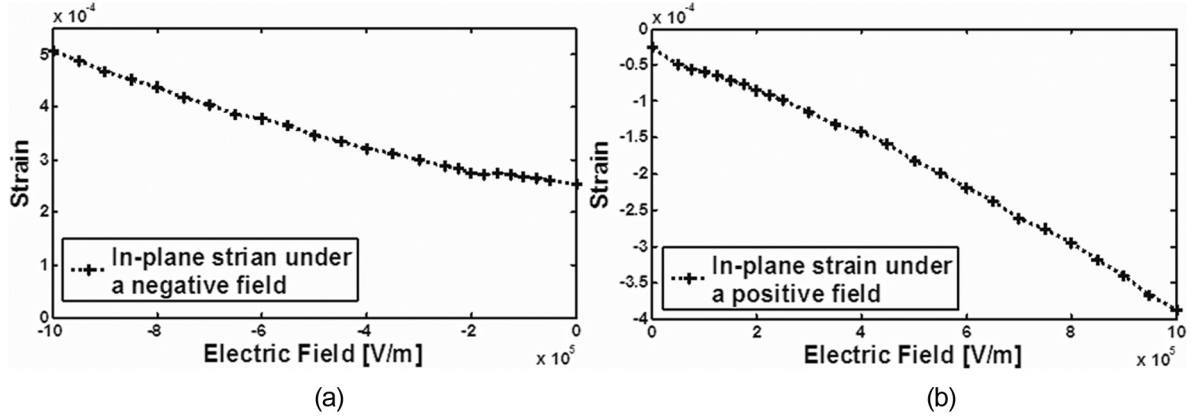
Figure 5. In-plane output strain of a bulk piezoelectric material when applied by a DC electric field: (a) in-plane output strain when applied by a negative DC electric field and (b) in-plane output strain when applied by a positive DC electric field. The initial strain offsets can obviously be seen in both polarities.

Table 2. The nonlinear d_{31} properties under positive and negative fields with initial strain offset in the PZT assigned in the model.

Polarity	$d_{31nonli}$ (m/V)	100% Initial strain in the PZT	Initial strain in the PZT assigned in the model
Positive	-18.8082×10^{-17}(E)-2.6516×10^{-10}	-2.6399×10^{-5}	-2.6399×10^{-5}
Negative	2.699×10^{-16}(E)-1.2040×10^{-10}	2.525×10^{-4}	1.2625×10^{-4}(reduced)

PZT: piezoelectric transducers.
"E" is the electric field. The column "100% initial strain in the PZT" represents a full residual strain offset. The column "Initial strain in the PZT assigned in the model" represents the reduced initial strain as assigned in the model.

(Figure 5(b)). Since it is more difficult for the domain walls to reorient back when they have been oriented opposing their polarization direction, fewer 90° domain wall orientations tend to occur under the positive field compared to the negative field. This results in a less pronounced permanent strain offset.

Experimental results of static testing of LIPCAs

The permanent residual displacements clearly appear in all the actuators for both charging conditions. The displacement offset had a large influence on the actuators' performance under the negative field, regardless of the discharging or non-discharging condition (Figures 6 to 11). The explanation of larger magnitude of permanent displacement offset under the negative field is explained in the preceding section.

It was observed that the permanent displacement offset was minimal under positive potential with a non-discharging condition (Figures 6(left) and 8(left)). The cause of the minimal permanent displacement offset can be explained as all the actuators being actuated the first time under a positive polarity and a non-discharging condition, which gives a low amount of 90° domain wall orientations compared to actuation under a negative polarity and non-discharging condition

(Figures 6(right) and 8(right)). A difference in a permanent offset can be seen when comparing [G/PZT/G/C/G/C] Figures 10(left) to 6(left) and 8(left). The layup [G/PZT/G/C/G/C], Figure 10(left), shows a larger amount of permanent displacement offset under a positive potential with the non-discharging condition. These different responses arise from the increased amount of irreversible 90° domain wall orientations of the layup [G/PZT/G/C/G/C]; compared to the other two layups, the first time layup [G/PZT/G/C/G/C] was actuated. This was because the piezoelectric material layer in the layup [G/PZT/G/C/G/C] was under more tensile stress than in the other two layups under a positive potential (Figure 18).

The common behavior of all the actuators was that all the actuation displacements were repeatable from the second experiment onward indicating that the permanent displacement offset resulting from 90° domain walls occurred only once. It was observable that the actuators exhibited the permanent displacement offsets similar to the initial strain offset that arise inside a bulk piezoelectric material (Figure 5). It can be observed that all the actuators clearly showed permanent displacements offset under the positive discharged condition (Figures 7(left), 9(left), and 11(left)) and the negative non-discharged (Figures 6(right), 8(right), and 10(right)) and discharged conditions (Figures 7(right),
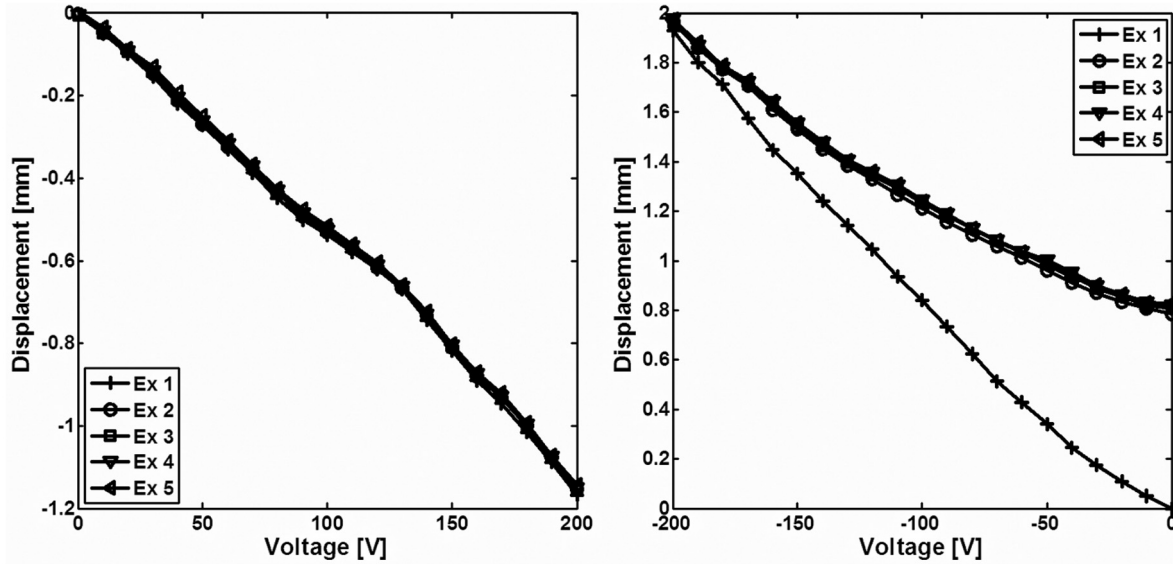
Figure 6. Static actuation displacement of [G/PZT/G/C] when the actuator was not discharged prior to the application of the next higher voltage under positive (left) and negative (right) fields. "Ex1" refers to experiment 1 and similarly for experiments 2 to 5.
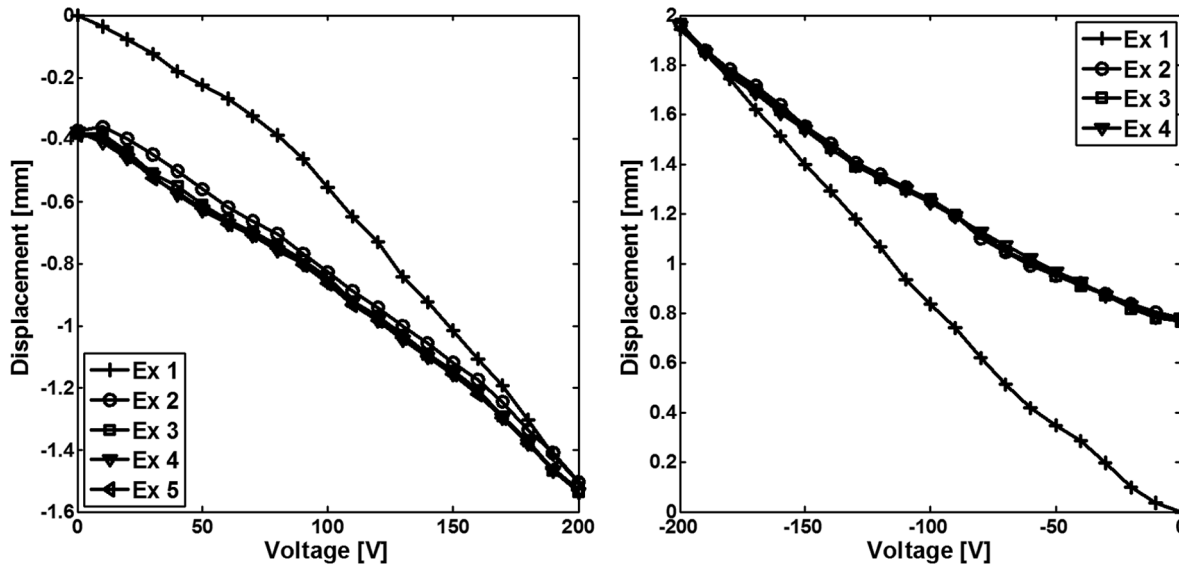
Figure 7. Static actuation displacement of [G/PZT/G/C] when the actuator was discharged prior to the application of the next higher voltage under positive (left) and negative (right) fields.

9(right), and 11(right)), indicating that regardless of the discharging or non-discharging condition of the actuators they all behaved similarly.

All the actuators exhibited nonlinear displacements as a result of a nonlinear piezoelectric response from a large input electric potential. The nonlinear displacement could be explained through the extrinsic effect described in the introduction. The true actuation displacements, displacement was subtracted by its initial displacement offset, of all the actuators from the second experiment onward were smaller than the true actuation displacements of the first experiment. This was caused by the 90° domain walls that were oriented irreversibly from the first experiment due to the large magnitude of input electric potential. Since a lot of 90° domain walls were already irreversibly oriented from the first experiment, there were fewer 90° domain walls left to contribute to the actuation displacement, leaving smaller true actuation displacements from the second experiment onward. The term true actuation displacement refers to the displacement without the permanent displacement offset.
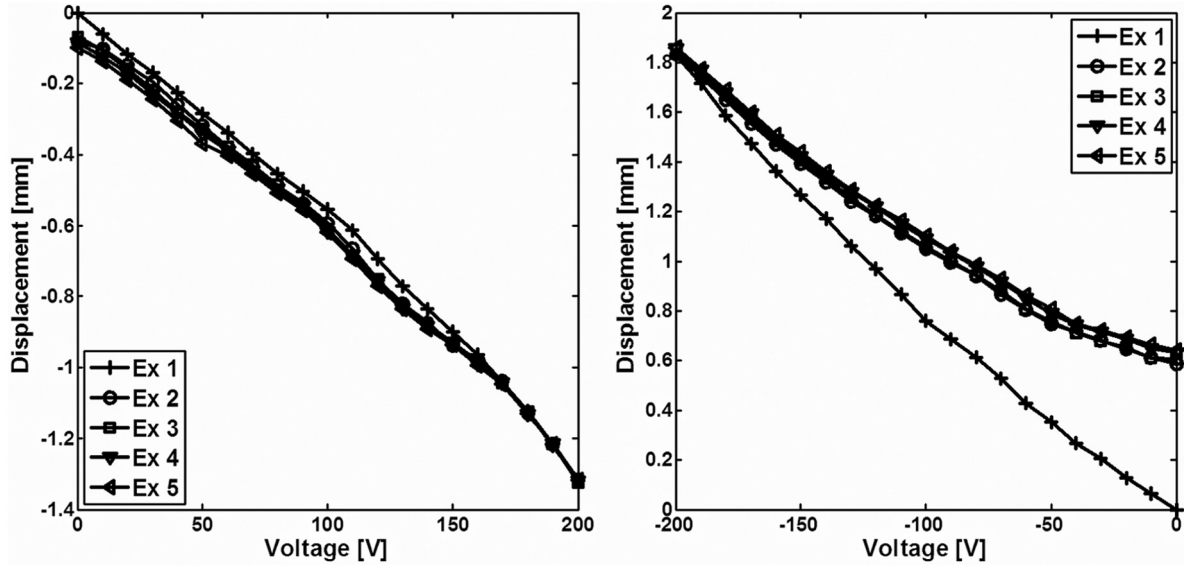
Figure 8. Static actuation displacement of [G/PZT/G/G/C] when the actuator was not discharged prior to the application of the next higher voltage under positive (left) and negative (right) fields.
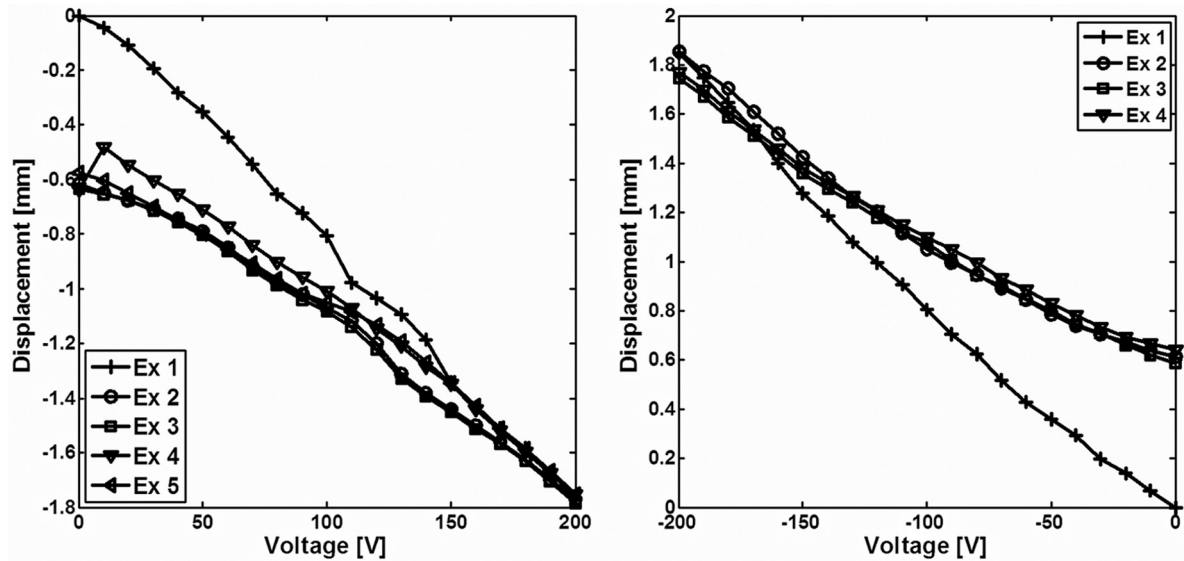
Figure 9. Static actuation displacement of [G/PZT/G/G/C] when the actuator was discharged prior to the application of the next higher voltage under positive (left) and negative (right) fields.

Experimental results versus finite element models

All actuators are required to operate more than one cycle in real applications and this causes permanent displacement offsets to exist. To replicate an actuator's actual behavior, the displacements from the second experiment onward were averaged and compared to the results of the models. This was because once the actuators were operated after the second experiment,

the actual displacement started from the permanent displacement offset.

The influence of the 90° domain wall orientations on the actuation response for all the three layups as shown from the displacement offsets is shown in Figures 12 to 14. The displacement offsets are similar to the initial strain offset inside a bulk piezoelectric material described in the "Nonlinear piezoelectric coefficients" section, while the displacement offset is larger. The
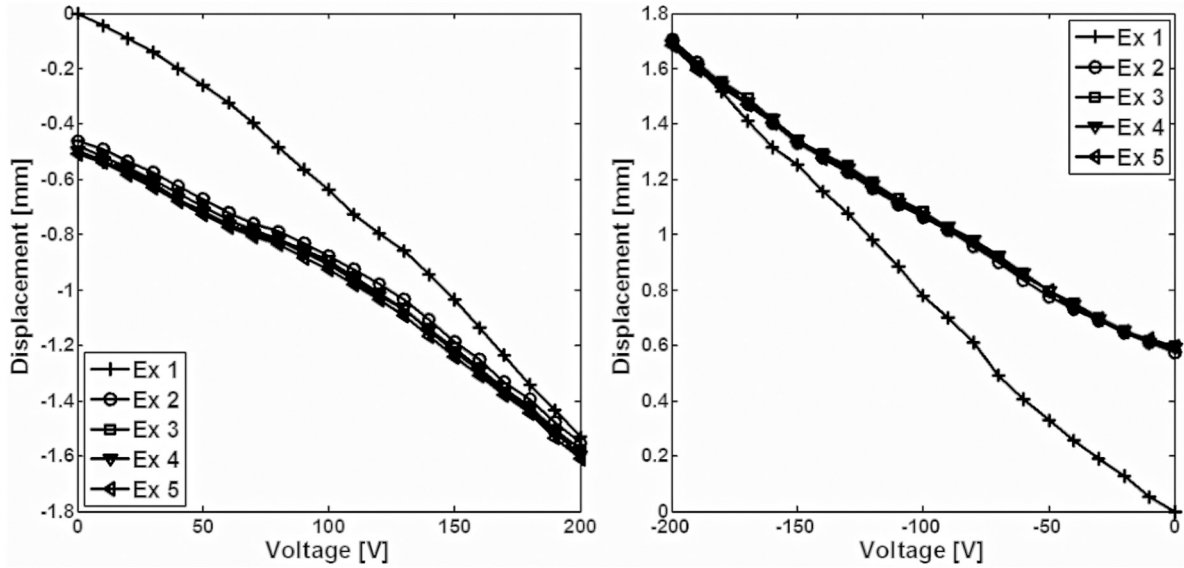
Figure 10. Static actuation displacement of [G/PZT/G/C/G/C] when the actuator was not discharged prior to the application of the next higher voltage under positive (left) and negative (right) fields.
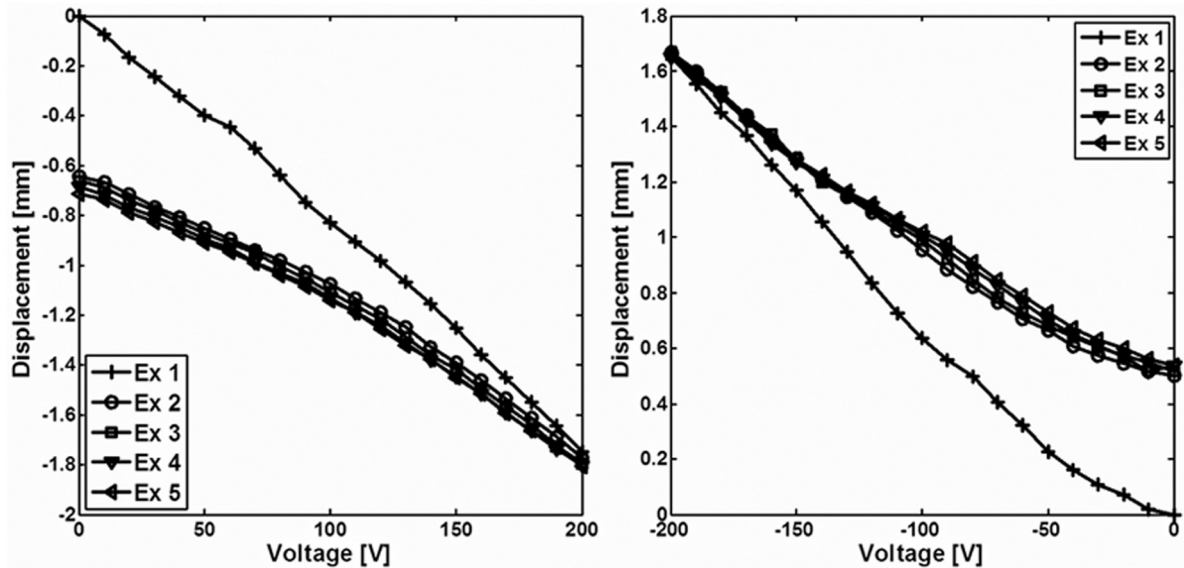
Figure 11. Static actuation displacement of [G/PZT/G/C/G/C] when the actuator was discharged prior to the application of the next higher voltage under positive (left) and negative (right) fields.

influence of the 90° domain wall orientations was more pronounced for the negative field than the positive one as explained in the previous section.

The "model linear" which incorporated a linear piezoelectric coefficient obtained from a manufacturer (see Table 1), which constitutes of only piezoelectric effects show only a linear relationship between input voltages and output displacements without permanent strain displacement offsets. The "model linear" failed to predict the actuation response in all cases because it lacked a description of the nonlinear piezoelectric behavior inside a linear piezoelectric coefficient due to small

electric field range used by the piezoelectric manufacturer. The small magnitude of the electric field used by the manufacturer did not include the effect of the 90° domain wall orientations but only the piezoelectric effect. The piezoelectric effect is the intrinsic effect, described in the introduction part; it is a linear response of the domain walls according to the application of a low magnitude electric field causing small and linear output strains.

The model "Model Nonlinear 100%strain" refers to the output displacements when a 100% permanent strain in the piezoelectric obtained from the experiments
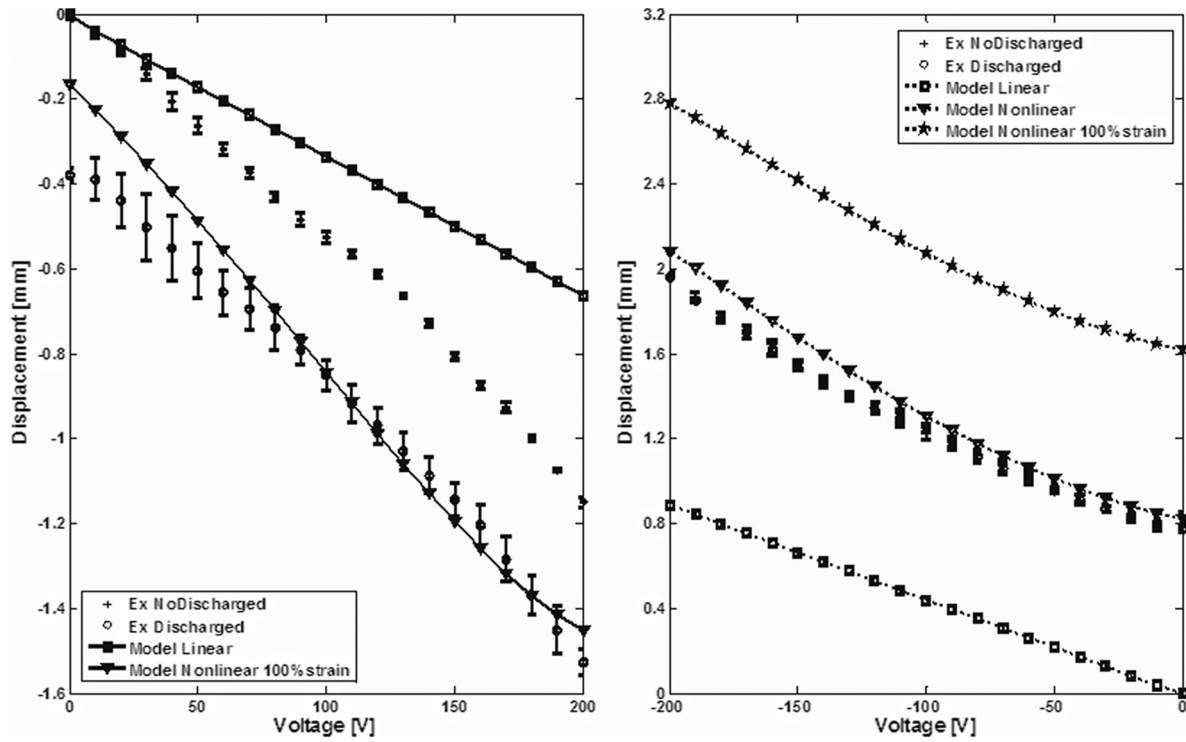
Figure 12. Experimental results of [G/PZT/G/C] under discharging and non-discharging conditions compared to the model with linear piezoelectric and nonlinear piezoelectric coefficients. "Ex Discharged" refers to the experimental results with a discharging condition. "Ex NoDischarged" refers to the experimental results without discharging the actuator. "Model Linear" refers to a model incorporates with a linear piezoelectric coefficient obtained from a manufacturer (Table 1). "Model Nonlinear" refers to a model incorporates with a nonlinear piezoelectric coefficient and initial strain to fit with the experimental results, column 4 in Table 2. The nonlinear piezoelectric coefficient was obtained when the piezoelectric material has been discharged but the initial strain remains inside the piezoelectric material. "Model Nonlinear 100%strain" refers to a model incorporates with a nonlinear piezoelectric coefficient with 100% initial strain resulting from 90° domain walls, column 3 in Table 2. Left: the actuator was actuated under a positive voltage. Right: the actuator was actuated under a negative voltage.
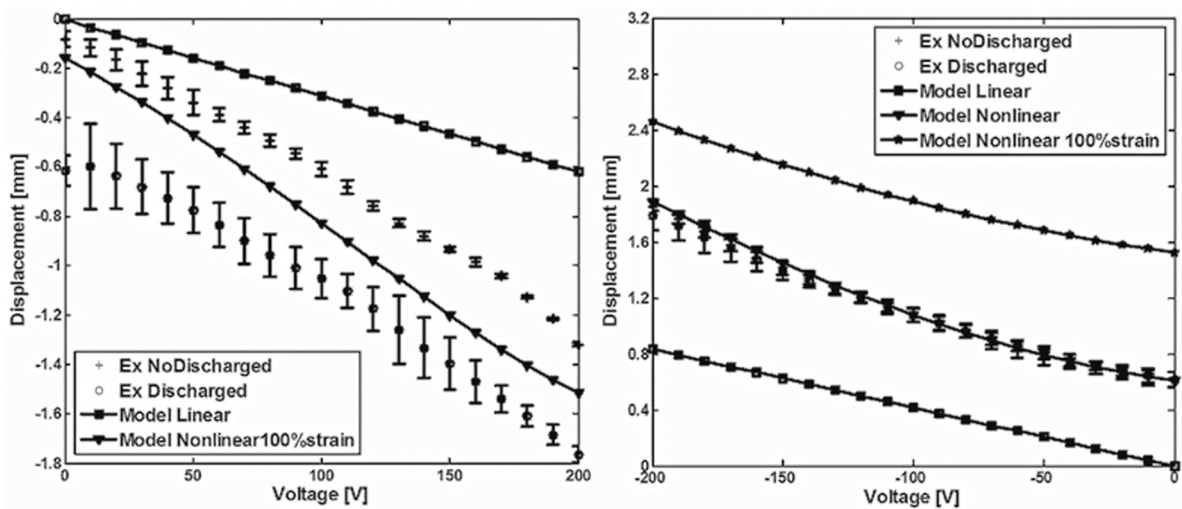
Figure 13. Experimental results of [G/PZT/G/G/C] under discharging and non-discharging conditions compared to the model with linear piezoelectric and nonlinear piezoelectric coefficients. The legend notations are similarly explained in Figure 11. Left: actuated under positive voltage. Right: actuated under negative voltage.

was included in the model. It was shown that with 100%strain, the output permanent displacements under a negative polarity were almost twice of the permanent displacement obtained experimentally. The predicted
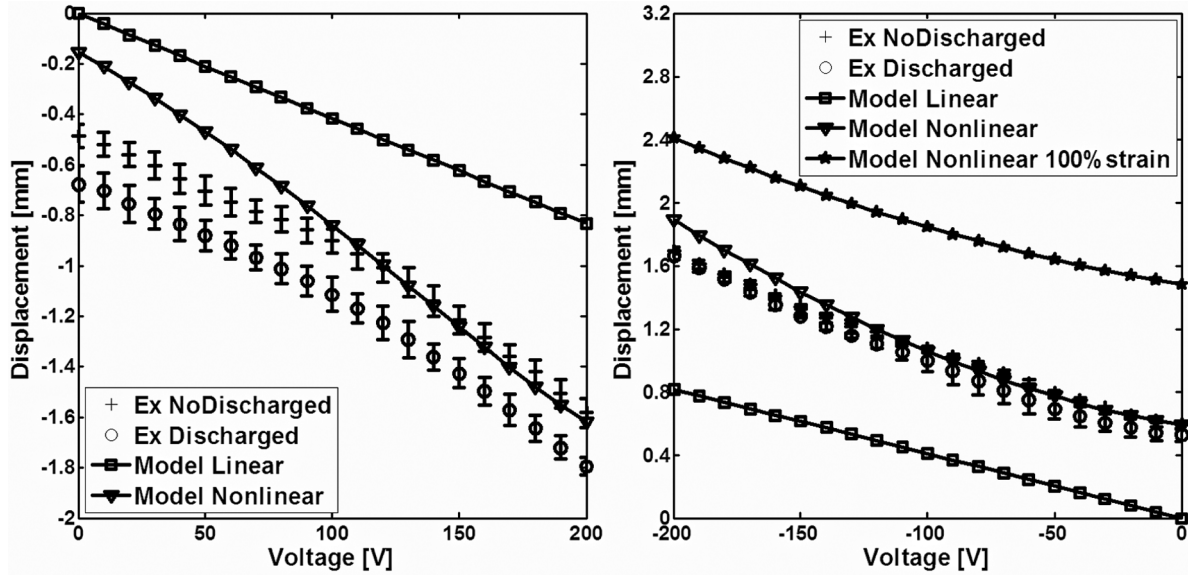
Figure 14. Experimental results of [G/PZT/G/C/G/C] under discharging and non-discharging conditions compared to the model with linear piezoelectric and nonlinear piezoelectric coefficients. The legend notations are similarly explained in Figure 12. Left: actuated under positive voltage. Right: actuated under negative voltage.

displacement offsets under a positive polarity, see "Model Nonlinear 100% strain," were somewhat smaller than the "Ex Discharged" experimental results for all the actuator layups. This was because the actuators were actuated under a discharging condition after they had gone through the non-discharging condition under both positive and negative polarity. Therefore, irreversible 90° domain wall orientations already existed inside the piezoelectric material under the discharging condition resulting in large permanent displacement offset when the actuators were actuated following the discharging testing condition. The predicted displacement offsets under a positive polarity were larger than the "Ex NoDischarged" experimental results for the actuator layups [G/PZT/G/G/C] and [G/PZT/G/C/G/C]. This could be explained by the experimental orders of all the actuators, that all the actuators were actuated for the first time after manufacturing under a positive potential and a non-discharging condition; thus, the amount of irreversible 90° domain walls arising inside these actuators were small; however, one can observe that the predicted displacement offsets under a positive polarity were smaller than the "Ex NoDischarged" experimental results for the layup [G/PZT/G/C/G/C]. This was because this particular layup experiences more tensile stress inside the piezoelectric material, resulting in more 90° domain wall orientations (Figure 18).

The model "Model Nonlinear," incorporates a reduced initial strain inside a piezoelectric material by 50% of the full strain (Table 2). The magnitude of 50% reduction was approximately made to match the initial displacement offsets of each actuator to the experimental results. The magnitude of 50% reduction

had to be approximately made because the true strain of the piezoelectric material inside a composite laminate is unknown. Although the offsets were not perfectly made in each individual layup, the 50% reduction provides a close approximation to the experiments. If the actuator were stiffer than the ones investigated for this article, the initial strain offsets would have been chosen to be lower than 50%. Under a negative potential, the permanent displacement offset starts at very close to the experimental value. This indicates that the permanent strain offset inside the piezoelectric material has been reduced by approximately half of the original value when embedded inside the composite laminate as shown in Table 2 and Figures 12 to 14. This is a result of the constraint from free expansion/contraction of the piezoelectric material inside the composite laminate.

Under a positive potential, the permanent strain offset was, instead of being reduced similarly to the negative potential case, amplified by tensile stress during actuation (Figures 15, 16, and 18). From Figure 15 it can be seen that at +200 V, the piezoelectric layer is under more tension than at +0 V, Figure 16 shows 90° domain walls are amplified when the piezoelectric layer is under tension. Hence, the initial strain in the piezoelectric layer under the positive potential is not reduced as the negative potential case. The tensile stress stretches the domain walls to form 90° domain walls, causing increased permanent strain offset in the piezoelectric material under a positive voltage.

When actuating under a negative potential, a compressive stress inside a piezoelectric layer causes reorientation of some of the domain walls back to their original orientation. This results in a lower permanent
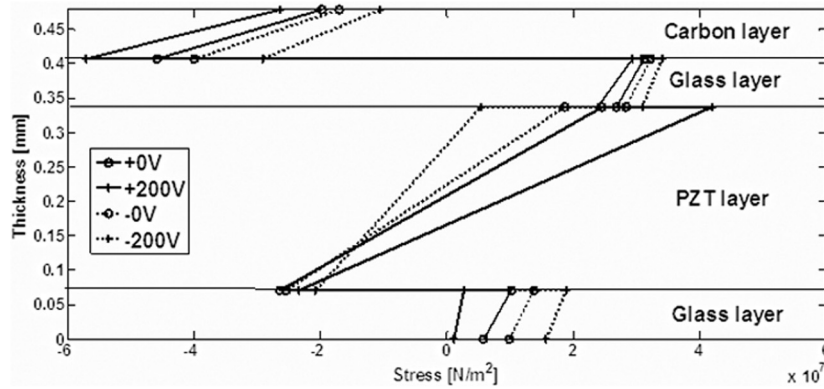
Figure 15. Changes of internal stress at the mid-length throughout thicknesses of [G/PZT/G/C] between 0 and ±200 V from COMSOL analysis. " + 0 V" refers to the stress condition at 0 V with initial strain obtained under positive electric field. "−0 V" refers to the stress condition at 0 V with reduced initial strain obtained under negative field.
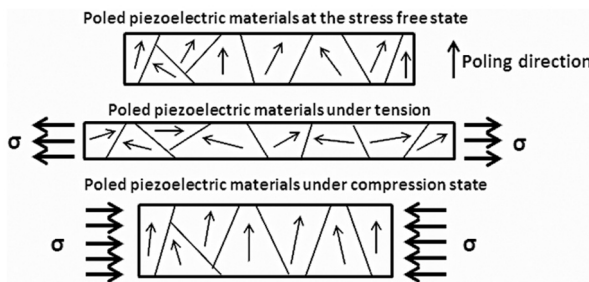
Figure 16. Illustration of how applied compression and tension stresses affect to the domains inside the bulk piezoelectric layer compared to the stress-free state.
Source: Adapted from Li et al. (1997).

displacement offset than a 100% strain offset could create, as illustrated in Figures 15 and 16.

As mentioned, tensile stress promotes more domain wall orientations, and the actuators experience more tensile stress when actuating under a positive potential; therefore, to produce a correct initial displacement offset under the positive potential, larger initial strain offsets should be applied to the piezoelectric coefficient (Figure 17). The corrected initial strains applied to each actuator layup are tabulated in Table 3. The actuator layup [G/PZT/G/C] had an approximately 200% increment in its initial stress, the actuator layup [G/PZT/G/G/C] had an approximately 300% increment in its initial stress, and the actuator layup [G/PZT/G/C/G/C] had an approximately 380% increment in its initial stress. The amount of increase in initial strain depends on how much the piezoelectric material experiences tensile stress. Taking the example of Figure 18, the layup [G/PZT/G/C] possess the smallest proportion of tensile stress throughout the piezoelectric material's thickness in relation to compressive stress when compared to the layups [G/PZT/G/G/C] and [G/PZT/G/C/G/C]. The layup [G/PZT/G/C/G/C] exhibits the largest

proportion of tensile stress throughout the piezoelectric material's thickness in relation to compressive stress than the other two layups; thus, more 90° domain wall orientations are promoted when compared to the other layups. Thus, the layup [G/PZT/G/C/G/C] requires more initial strain to correct the initial actuation displacement. In contrast, the reduced amount of strain under a negative potential, when the piezoelectric material is under more compression, is approximately similar in all actuator layups, that is, approximately 50% in all layups. This could explain the proportion of the tensile stress throughout the piezoelectric material's thickness of all actuator layups which were more than the proportion of the compressive stress. Thus, there is more influence of the tensile stress than the compressive stress.

The nonlinear actuation response is another major influence on actuator performance as can be seen from the actuation displacements at higher electric potential magnitudes, that is, most obviously starting from 50 V and higher. The actuators produce nonlinear actuation responses at this higher electric potential range and the model which uses the nonlinear piezoelectric coefficient can pick up this phenomenon better than the model using a linear piezoelectric coefficient. The model using a linear piezoelectric coefficient was not able to predict this phenomenon.

Understanding the actuator performance

In the previous sections, the repeatability of all the actuators responses, the asymmetry of the actuation response between positive and negative potentials compared to the models was discussed. In this section, parameters influencing the differences in actuation response from different layups will be discussed. Combining Figures 6, 8, and 10, we get Figure 19. Combining Figures 7, 9, and 11, we get Figure 20. Figures 19 and 20 clearly show the asymmetry of the
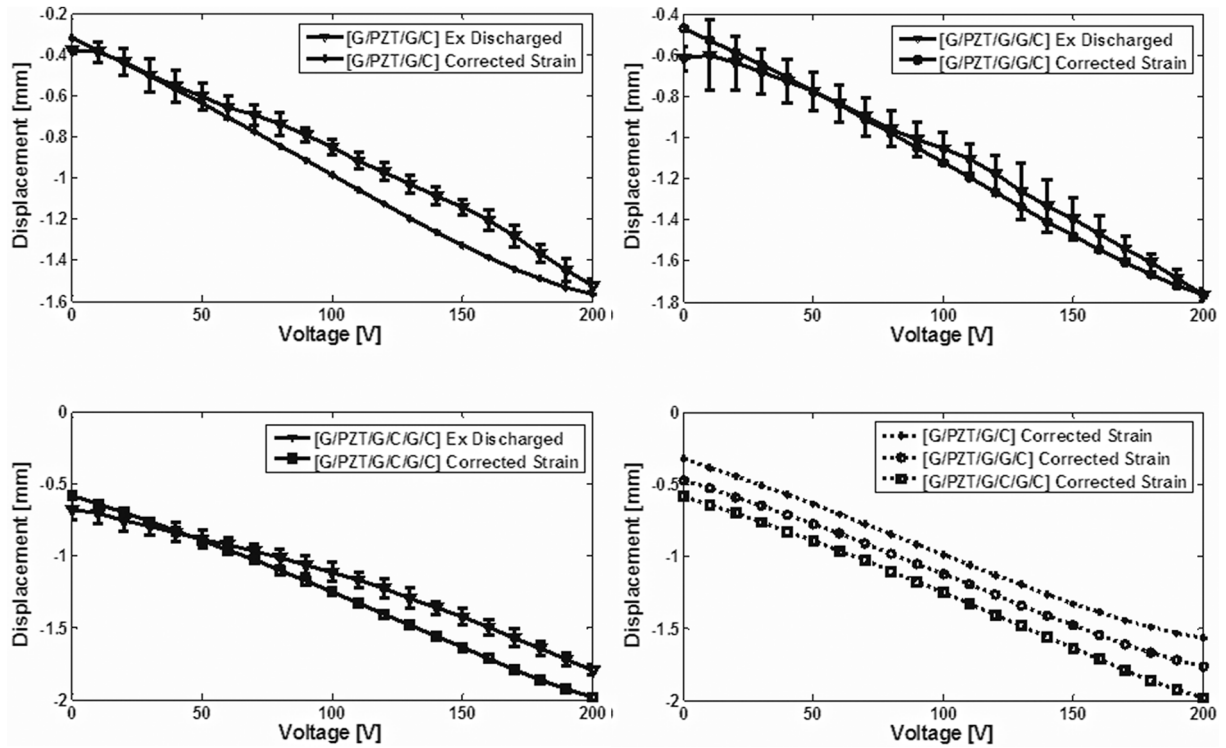
Figure 17. Predicted actuation displacements with corrected initial strain versus experimental results under a discharging condition under the positive polarity.

Table 3. Corrected initial strain applied to the piezoelectric material under a positive potential.

Actuator layups	Corrected initial strain
[G/PZT/G/C]	−5.28E-05
[G/PZT/G/G/C]	−8.00E-05
[G/PZT/G/C/G/C]	−10.0E-05

actuation response of all the actuators between the two polarities under both charging conditions.

Although there was some variation in the displacement offset under the positive field between the discharged and the non-discharged cases, the trends of the actuation performances of all the layups were similar under both polarities. This indicates that regardless of having the actuators discharged or not discharged prior
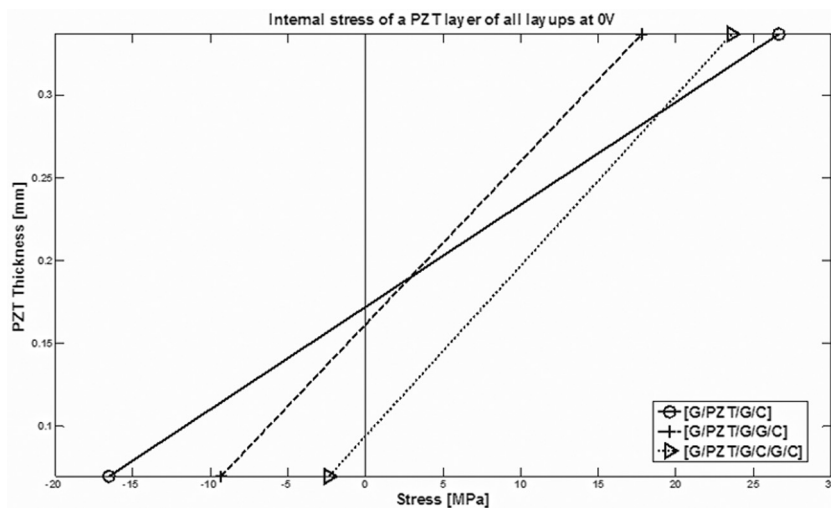
Figure 18. Internal stress throughout the piezoelectric thickness at 0 V or after the manufacturing process.
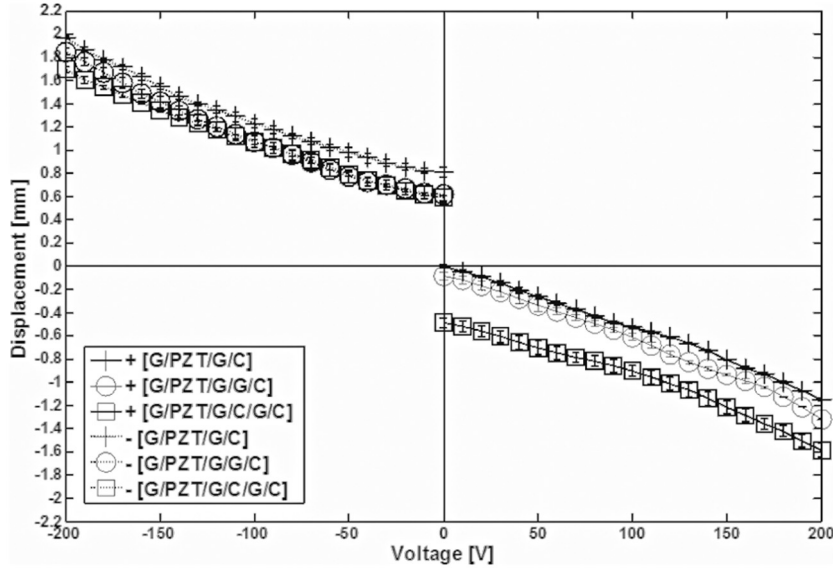
Figure 19. Experimental results of all actuators under both positive and negative voltages when the actuators were not discharged prior to the application of the next higher voltage.
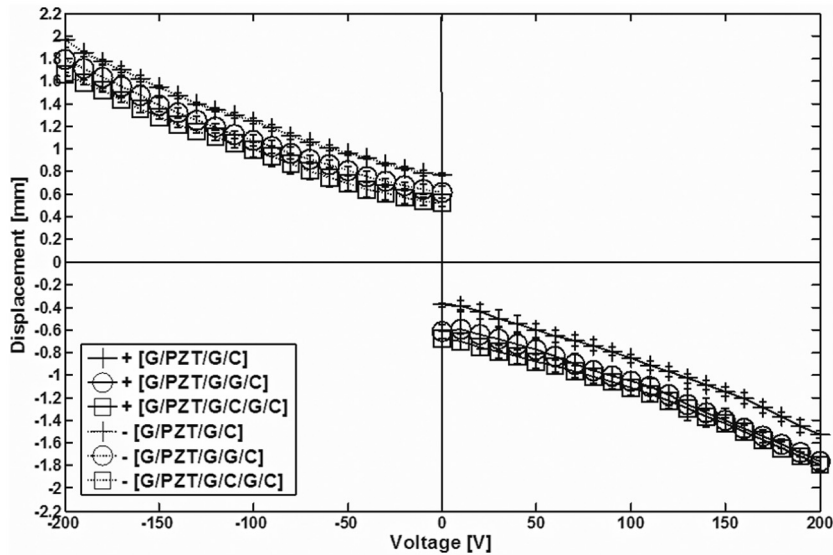
Figure 20. Experimental results of all actuators under both positive and negative voltages when the actuators were discharged prior to the application of the next higher voltage.

to the next higher electric potential, the displacement offset due to 90° domain wall orientations remained. This is due to the piezoelectric material being restricted from free movement as it was embedded in a composite laminate and the 90° domain walls had been irreversibly oriented. Therefore, its strain state could not be diminished to zero strain even under a discharging condition.

To investigate the actuation response without the influences of the permanent displacement offset, the actuation displacements were adjusted to the zero displacement by subtracting the actuation displacement from the displacement offset of each individual actuator within each individual polarity. The result is shown in Figure 21. It can be observed that without the permanent displacement offsets, all the actuators behaved similarly. When comparing of Figures 21 and 22, where the linear piezoelectric coefficient given by the manufacturer was incorporated into the model, it is clearly seen that these actuators behave similarly in a small electric potential range, that is, $\leq \pm 50$ V as defined within this study. Within a small electric field range, all the actuators behaved indistinguishable, that is, there was no influence from the different layups; however, the actuation displacement magnitudes were
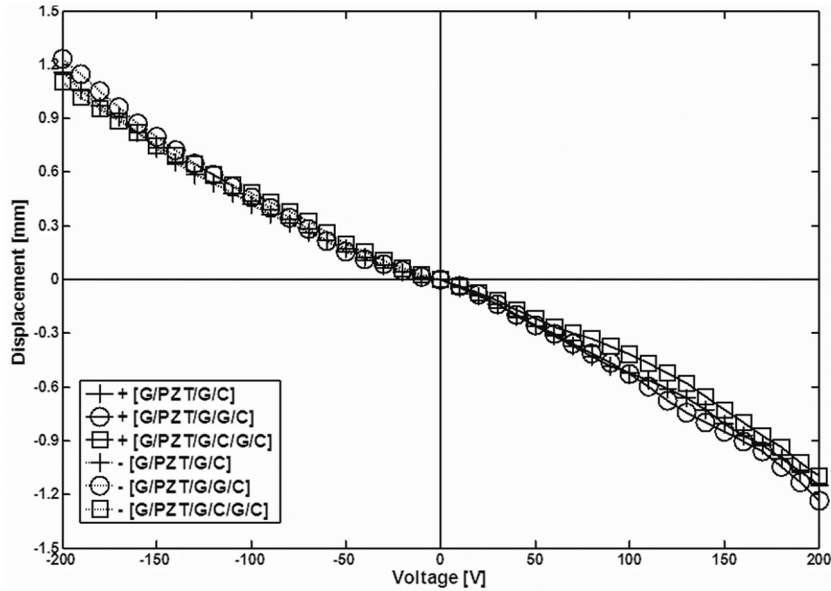
Figure 21. Experimental results of all actuator, when all of the permanent displacement offsets were deducted, under both positive and voltages when the actuators were discharged prior to the application of the next higher voltage.
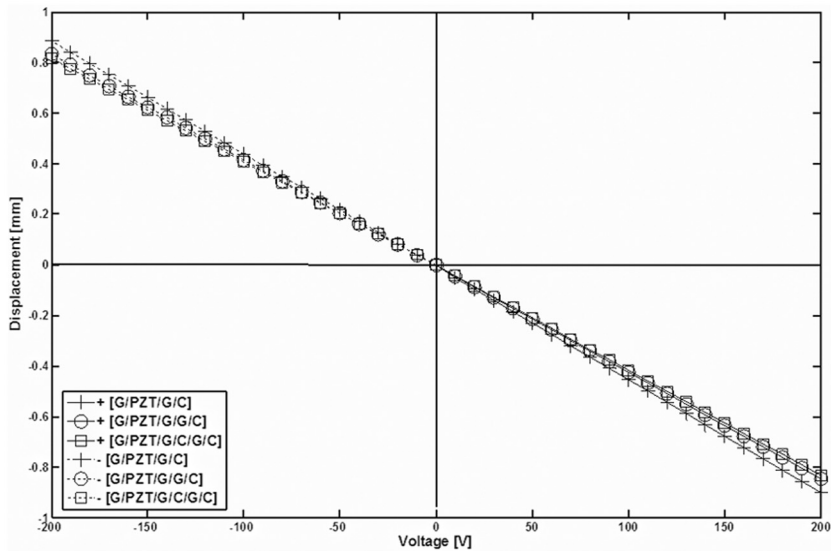
Figure 22. Actuation displacements of all actuator layups when a linear piezoelectric coefficient is incorporated into the model.

clearly different in a larger electric potential range, that is, more than ±50 V, due to the nonlinear response of the piezoelectric material. As studied by Li et al. (1991), a linear piezoelectric effect is produced in a field level of as low as 10 V/mm. The 50 V input voltage used in these actuators is approximately as large as 180 V/mm. Within the transition between the small and large electric potential range, between ±50 and ±100 V defined in this study, an actuators' performance starts to be distinguishable. Considering the large electric potential range, >±100 V defined in this study, the individual layup showed difference in their actuation responses and the displacements were nonlinear. This indicated that without a permanent

displacement offset, the nonlinearity of the piezoelectric response causes differences in the actuation response of individual layups (Figure 21). Nevertheless, the large input electric potential range presented still shows less influence due to the actuation response from different layups compared to the large impact of the permanent displacement offset (see Figures 20 and 21). The predicted actuation displacements with corrected initial strain of all layups, denoted as "Model Nonlinear" from Figures 12(right), 13(right) to 14(right) and a lower right figure in Figure 17 are combined and become Figure 23. It can be observed that the actuation displacements obtained from the model with corrected initial strain to match with the experimental results
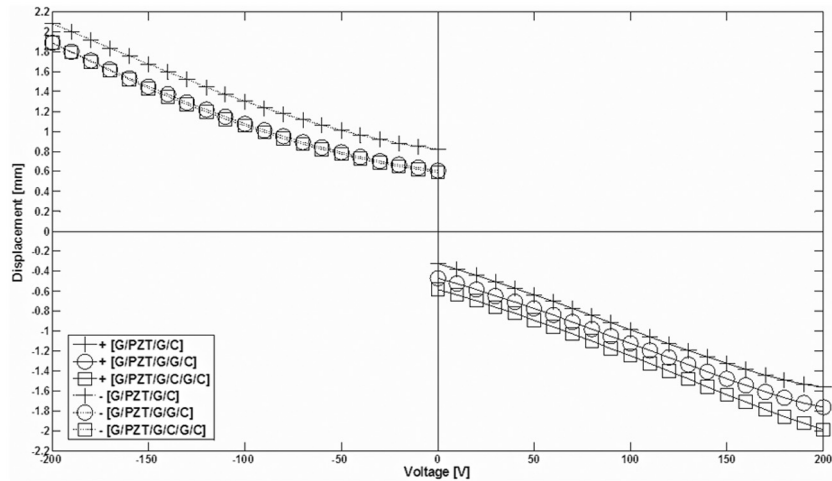
Figure 23. Predicted actuation displacements with corrected strain.

under a discharging condition (Figure 23), show well agreement with the actual actuation displacement trends under a discharging condition (Figure 20).

Conclusion

The actuators were actuated under two DC electric polarities and charging conditions, and they were actuated in more than one experiment per input DC electric polarity. The actuators' actuation response stabilized from the second experiment onward leaving a clearly permanent displacement offset after the first experiment. This indicated that the permanent displacement offset occurred only once. The experimental results showed that regardless of the charging condition prior the application of the next higher electric potential, the permanent displacement offsets were still present. This indicated that the permanent displacement offset resulting from the 90° domain wall orientations remained inside the piezoelectric layer in all charging conditions as long as the electric potential magnitude was large enough to cause irreversibility of the 90° domain walls.

Two finite element models were developed to predict the actuation response of three actuator layups: one model with a linear piezoelectric coefficient and another model with a nonlinear piezoelectric coefficient plus permanent strain offset remaining inside the piezoelectric material. It was shown that when the actuators were operated at a large input electric potential, the linear piezoelectric coefficient failed to predict the actuation response, while the nonlinear piezoelectric coefficient could pick up both permanent displacement offset and the nonlinear actuation response well.

It was further observed that the main parameter for the different behavior of the actuators' performance was the actuator's individual permanent displacement

offset and the second parameter for the different behavior was the nonlinear response of the piezoelectric material at larger potential. Finally, the piezoelectric material linear response did not contribute to the difference in the actuators' performance.

Declaration of Conflicting Interests

Funding

References

Aimmanee S and Hyer MW (2006) A comparison of the deformations of various piezoceramic actuators. *Journal of Intelligent Material Systems and Structures* 17(2): 167–186.

Antcliff RR and McGowan AMR (2001) Active control technology at NASA Langley Research Center. In: *Proceedings of the active control technology for enhanced performance operational capabilities of military aircraft, land vehicles and sea vehicles*, Braunschweig, 8–11 May 2000, pp. 1–13. Hampton, VA: NASA Langley Research Center.

Ballas RG (2007) *Piezoelectric Multilayer Beam Bending Actuators: Static and Dynamic Behavior and Aspects of Sensor Integration*. Berlin, Heidelberg: Springer-Verlag.

Goo NS, Kim C, Kwon YD, et al. (2001) Behaviors and performance evaluation of a lightweight piezo-composite curved actuator. *Journal of Intelligent Material Systems and Structures* 12(9): 639–646.

Hall DA (2001) Review: nonlinearity in piezoelectric ceramics. *Journal of Materials Science* 36(19): 4575–4601.

Jeronimidis G and Parkyn AT (1988) Residual stresses in carbon fiber-thermoplastic matrix laminates. *Journal of Composite Materials* 22(5): 401–415.

Li G, Furman G and Haertling HG (1997) Stress-enhanced displacements in PLZT rainbow actuators. *Journal of the American Ceramic Society* 80(6): 1382–1388.

Li S, Cao W and Cross LE (1991) The extrinsic nature of nonlinear behavior observed in lead zirconate titanate ferroelectric ceramic. *Journal of Applied Physics* 69(10): 7219–7224.

Mossi KM, Selby GV and Bryant RG (1998) Thin-layer composite unimorph ferroelectric driver and sensor properties. *Materials Letters* 35(1–2): 39–49.

Pramanick A, Damjanovic D, Daniels JE, et al. (2011) Origins of electro-mechanical coupling in polycrystalline ferroelectrics during subcoercive electrical loading. *Journal of the American Ceramic Society* 94(2): 293–309.

Pramanick A, Damjanovic D, Nino JC, et al. (2009) Subcoercive cyclic electrical loading of lead zirconate titanate ceramics I: nonlinearities and losses in the converse piezoelectric effect. *Journal of the American Ceramic Society* 92(10): 2291–2299.

Standards Committee of the IEEE Ultrasonics, Ferroelectrics, and Frequency Control Society (1988) *IEEE Standard on Piezoelectricity*. New York: IEEE.

Wiwattananon P, Ahmed TJ, Hulskamp AW, et al. (2009) Investigation of a thermoplastic alternative for LIPCA. In: *Proceedings of the 20th international conference on adaptive structures and technologies*, Hong Kong, *20–22 October*.

Wiwattananon P, Bergsma OK and Bersee HEN (2011) Nonlinear finite-element model of piezoelectric composite-based actuator. In: *Proceedings of the 22nd international conference on adaptive structures and technologies*, Corfu, 10–12 October.

Yoon KJ, Seokjun S, Hoon CP, et al. (2002) Design and manufacture of a lightweight piezo-composite curved actuator. *Smart Materials and Structures* 11(1): 163.